

# Widely Linear Adaptive Frequency Estimation In Three-Phase Power Systems Under Unbalanced Voltage Sag Conditions

Yili Xia, Scott C. Douglas, and Danilo P. Mandic

**Abstract**—A new framework for the estimation of the instantaneous frequency in a three-phase power system is proposed. It is first illustrated that the complex-valued signal, obtained by the  $\alpha\beta$  transformation of three-phase power signals under unbalanced voltage sag conditions, is second order noncircular, for which standard complex adaptive estimators are suboptimal. To cater for second order noncircularity, an adaptive widely linear estimator based on the augmented complex least mean square (ACLMS) algorithm is proposed, and the analysis shows that this allows for optimal linear adaptive estimation for the generality of system conditions (both balanced and unbalanced). The enhanced robustness over the standard CLMS is illustrated by simulations on both synthetic and real-world voltage sags.

## I. INTRODUCTION

In a power system, unexpected frequency variations from the nominal value can trigger abnormal system conditions and disturbances, and fast and accurate frequency estimation has recently attracted much attention [1], [2]. Standard single phase based techniques are limited, especially when the selected phase suffers a dip in voltage or transients. It is also difficult to select the most representative single-phase signal to adequately describe the system frequency, since six different single-phase voltages exist in a three-phase system, when line-to-line voltages are also considered [3]. Therefore, an optimal solution would be to design a framework which simultaneously considers all the three-phase voltages; this provides unified estimation with enhanced robustness whenever any of the phases suffers sags, transients or harmonics. To this end, Clarke's  $\alpha\beta$  transformation constructs a complex-valued signal from the information provided by all the three-phase voltages [4]. This transformation equips classical single phase methods with enhanced robustness, and a number of solutions have been developed in the complex domain  $\mathbb{C}$  that have proved more reliable than the corresponding methods operating in the real domain  $\mathbb{R}$ . These include the use of phase locked loops (PLL) [5], least squares techniques [6], Kalman filtering [7], and demodulation based methods [8]. Among them, adaptive algorithms based on the minimisation of the mean square error are most widely used, owing to their simplicity, computational efficiency, and robust performance for frequency estimation in the presence of noise and harmonic distortions.

In real-world distributed power systems, one main problem are unbalanced voltage sags triggered by an increase in load current that may last from a period of one cycle to a few

hundred cycles of the AC source [9]. Such a short-term increase in load currents may occur due to motor starting, transformer inrush, short circuits, or fast reclosing of circuit breakers. Despite their short duration, such unbalanced events may cause difficulties in phase angle calculation when using standard adaptive estimators. This problem has been discussed in [10], where the complex-valued signal obtained from an unbalanced three-phase voltage source was represented as an orthogonal sum of positive and negative sequences. Since the standard complex linear adaptive filter can only cater for the positive sequences, the negative sequences introduce a systemic estimation error oscillating at twice the system frequency [11]; attempts to estimate frequency under unbalanced conditions can be found in [12], [13].

Based on recent advances in augmented complex-valued second order statistics, we illustrate that under unbalanced conditions, the complex-valued signal obtained from the  $\alpha\beta$  transformation is second order noncircular (improper), for which the probability density function is not rotation invariant. The so-called augmented complex statistics show that for the modelling of noncircular signals, the standard linear estimation, based on the covariance matrix of a complex-valued random vector  $\mathbf{x}$ , that is  $\mathbf{C}_{\mathbf{xx}} = E[\mathbf{xx}^H]$ , is not adequate and the pseudocovariance matrix  $\mathbf{P}_{\mathbf{xx}} = E[\mathbf{xx}^T]$  should also be taken into account to describe the complete second order behaviour [14], [15]. In practice, this is achieved by virtue of the widely linear modelling [14], [16], where both  $\mathbf{x}$  and its complex conjugate  $\mathbf{x}^*$  are combined into the augmented input  $\mathbf{x}_a = [\mathbf{x}^T, \mathbf{x}^H]^T$ . To deal with online frequency estimation on noncircular signals, we here propose to use the recently introduced widely linear modelling based adaptive filtering algorithm, called the Augmented Complex Least Mean Square (ACLMS) [17]. Its superiority over standard CLMS [6] is illustrated by analysis and simulations over several typical synthetic and real world unbalanced voltage sag conditions.

## II. PRELIMINARIES

### A. Widely Linear Modelling

Consider a real-valued conditional mean squared error (MSE) estimator

$$\hat{y} = E[y|x] \quad (1)$$

which estimates the signal  $y$  in terms of another observation  $x$ . For zero mean, jointly normal  $y$  and  $x$ , the optimal solution is the linear model given by

$$\hat{y} = \mathbf{x}^T \mathbf{h} \quad (2)$$

Y. Xia and D. P. Mandic are with the Department of Electrical and Electronic Engineering, Imperial College London, London, UK. (e-mail: yili.xia06, d.mandic@imperial.ac.uk).

S. C. Douglas is with Department of Electrical Engineering, Southern Methodist University, Dallas, USA. (e-mail: douglas@engr.smu.edu).

where  $\mathbf{h} = [h_1, \dots, h_L]^T$  is a vector of fixed filter coefficients,  $\mathbf{x} = [x_1, \dots, x_L]^T$  the regressor vector, and  $(\cdot)^T$  the vector transpose operator.

In the complex domain, it is typically assumed that we can use the same form of estimator, leading to the standard complex linear minimum mean square error (MMSE) estimator

$$\hat{y} = \hat{y}_r + j\hat{y}_i = \mathbf{x}^T \mathbf{h} \quad (3)$$

where  $j = \sqrt{-1}$  and subscripts  $r$  and  $i$  denote respectively the real and imaginary parts of a complex variable. Since both the real and imaginary parts of complex variables are real, we have

$$\hat{y}_r = E[y_r|x_r, x_i], \quad \hat{y}_i = E[y_i|x_r, x_i] \quad (4)$$

and a more general form of (3) becomes

$$\hat{y} = E[y_r|x_r, x_i] + jE[y_i|x_r, x_i] \quad (5)$$

Substitute  $x_r = (x + x^*)/2$  and  $x_i = (x - x^*)/2j$  to arrive at

$$\hat{y} = E[y_r|x, x^*] + jE[y_i|x, x^*] = E[y|x, x^*] \quad (6)$$

leading to the *widely linear* estimator for complex valued data

$$\hat{y} = \mathbf{h}^T \mathbf{x} + \mathbf{g}^T \mathbf{x}^* = \mathbf{x}^T \mathbf{h} + \mathbf{x}^H \mathbf{g} \quad (7)$$

where  $\mathbf{h}$  and  $\mathbf{g}$  are complex-valued coefficient vectors. Such a widely linear estimator is optimal for the generality of complex signals (both proper and improper), and it simplifies into the strictly linear model ( $\mathbf{g} = \mathbf{0}$ ) for proper data.

### B. Augmented complex statistics

In practice, the widely linear estimate in (7) is based on a regressor vector produced by concatenating the input vector  $\mathbf{x}$  with its conjugate  $\mathbf{x}^*$ , to give an augmented  $2L \times 1$  input vector  $\mathbf{x}^a = [\mathbf{x}^T, \mathbf{x}^{H}]^T$ , together with the corresponding augmented coefficient vector  $\mathbf{w}^a = [\mathbf{h}^T, \mathbf{g}^T]^T$ . The corresponding  $2L \times 2L$  augmented covariance matrix then becomes [15]

$$\mathbf{C}_{\mathbf{x}^a} = E \begin{bmatrix} \mathbf{x} \\ \mathbf{x}^* \end{bmatrix} [\mathbf{x}^H \mathbf{x}^T] = \begin{bmatrix} \mathbf{C}_{\mathbf{x}\mathbf{x}} & \mathbf{P}_{\mathbf{x}\mathbf{x}} \\ \mathbf{P}_{\mathbf{x}\mathbf{x}}^* & \mathbf{C}_{\mathbf{x}\mathbf{x}} \end{bmatrix} \quad (8)$$

and contains the full second order statistical information. From (8), it is clear that the covariance matrix,  $\mathbf{C}_{\mathbf{x}\mathbf{x}} = E[\mathbf{x}\mathbf{x}^H]$ , alone does not have sufficient degrees of freedom to describe full second order statistics, and in order to make use of all the available second order information we also need to consider the pseudo-covariance matrix,  $\mathbf{P}_{\mathbf{x}\mathbf{x}} = E[\mathbf{x}\mathbf{x}^T]$ . Processes with the vanishing pseudo-covariance,  $\mathbf{P}_{\mathbf{x}\mathbf{x}} = \mathbf{0}$ , are termed second order circular (or proper). In general, the notion of circularity extends beyond second order statistics, to describe the class of signals with rotation-invariant distributions,  $\mathcal{P}[\cdot]$  for which  $\mathcal{P}[\mathbf{z}] = \mathcal{P}[\mathbf{z}e^{j\theta}]$  for  $\theta \in [0, 2\pi)$  [18]. In real world, most complex signals are second order noncircular or improper, and their probability density functions are not rotation invariant. Fig. 1 shows the scatter plots of some complex-valued signals [19]. Note that the distribution of a stable AR(4) signal driven by the circular doubly white Gaussian noise is circularly symmetric, and becomes noncircular for improper driving

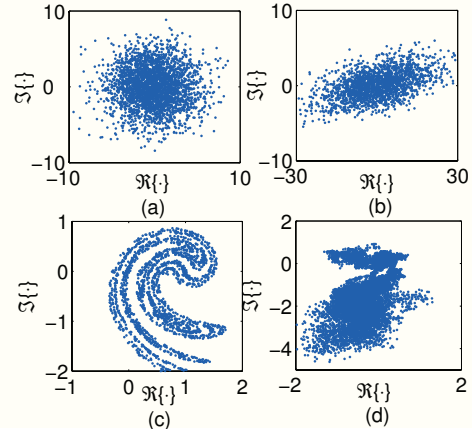


Fig. 1. Circularity via “real-imaginary” scatter plots in the complex plane. (a) A stable autoregressive AR(4) process driven by doubly white circular Gaussian noise. (b) The same AR(4) process driven by noncircular doubly white Gaussian noise. (c) Noncircular Ikeda map. (d) Real-world wind signal.

noise, as shown in Fig. 1(b). The noncircularity can also be seen in the chaotic Ikeda map and real-world wind data<sup>1</sup>.

The advantage of widely linear estimation over strictly linear estimation can be quantified by the difference between the mean square errors of a strictly linear estimator,  $e_L^2$ , and that of a widely linear estimator,  $e_{WL}^2$  [14], given by

$$\begin{aligned} \delta e^2 &= e_L^2 - e_{WL}^2 \\ &= [\mathbf{p} - \mathbf{P}_{\mathbf{x}\mathbf{x}}^* \mathbf{C}_{\mathbf{x}\mathbf{x}}^{*-1} \mathbf{c}^*]^H [\mathbf{C}_{\mathbf{x}\mathbf{x}} - \mathbf{P}_{\mathbf{x}\mathbf{x}} \mathbf{C}_{\mathbf{x}\mathbf{x}}^{*-1} \mathbf{P}_{\mathbf{x}\mathbf{x}}^*]^{-1} \\ &\quad \cdot [\mathbf{p} - \mathbf{P}_{\mathbf{x}\mathbf{x}}^* \mathbf{C}_{\mathbf{x}\mathbf{x}}^{*-1} \mathbf{c}^*] \end{aligned} \quad (9)$$

where  $\mathbf{c} = E[y^* \mathbf{x}]$  and  $\mathbf{p} = E[y \mathbf{x}]$ . Due to the positive definiteness of the matrix  $[\mathbf{C}_{\mathbf{x}\mathbf{x}} - \mathbf{P}_{\mathbf{x}\mathbf{x}} \mathbf{C}_{\mathbf{x}\mathbf{x}}^{*-1} \mathbf{P}_{\mathbf{x}\mathbf{x}}^*]$ ,  $\delta e^2$  is nonnegative.

### III. FREQUENCY ESTIMATION BASED ON WIDELY LINEAR ADAPTIVE FILTERING

The three-phase voltages of a power system in a noise-free environment can be represented in a discrete time form as

$$\begin{aligned} v_a(k) &= V_a(k) \cos(\omega k \Delta T + \phi) \\ v_b(k) &= V_b(k) \cos(\omega k \Delta T + \phi - \frac{2\pi}{3}) \\ v_c(k) &= V_c(k) \cos(\omega k \Delta T + \phi + \frac{2\pi}{3}) \end{aligned} \quad (10)$$

where  $V_a(k), V_b(k), V_c(k)$  are the peak values of each phase voltage component at time instant  $k$ ,  $\Delta T$  the sampling interval,  $\phi$  the phase of fundamental component, and  $\omega = 2\pi f$  the angular frequency of the voltage signal, with  $f$  being the system frequency. The time-dependent three-phase voltage is transformed by the orthogonal  $\alpha\beta 0$  transformation matrix [4] into a zero-sequence  $v_0$  and the direct and quadrature-axis components,  $v_\alpha$  and  $v_\beta$ , as

$$\begin{bmatrix} v_0(k) \\ v_\alpha(k) \\ v_\beta(k) \end{bmatrix} = \sqrt{\frac{2}{3}} \begin{bmatrix} \frac{\sqrt{2}}{2} & \frac{\sqrt{2}}{2} & \frac{\sqrt{2}}{2} \\ 1 & -\frac{1}{2} & -\frac{1}{2} \\ 0 & \frac{\sqrt{3}}{2} & -\frac{\sqrt{3}}{2} \end{bmatrix} \begin{bmatrix} v_a(k) \\ v_b(k) \\ v_c(k) \end{bmatrix} \quad (11)$$

<sup>1</sup>The wind signal was made complex through combining the wind speed  $v$  and direction  $\psi$  to form a complex signal  $\mathbf{v} = ve^{j\psi}$ .

The factor  $\sqrt{2/3}$  is used to ensure that the system power is invariant under this transformation. When  $V_a(k), V_b(k), V_c(k)$  are identical,  $v_0(k) = 0$ ,  $v_\alpha(k) = A\cos(\omega k\Delta T + \phi)$  and  $v_\beta(k) = A\cos(\omega k\Delta T + \phi + \frac{\pi}{2})$ , with a constant amplitude  $A$ , while  $v_\alpha(k)$  and  $v_\beta(k)$  are the orthogonal coordinates of a point whose position is time variant at a rate proportional to the system frequency.

In practice, only the  $v_\alpha$  and  $v_\beta$  parts are used in the modelling, known as the  $\alpha\beta$  transformation [8]. The resulting complex voltage signal  $v(k)$  serves as the desired signal in adaptive frequency estimation and is given by

$$v(k) = v_\alpha(k) + jv_\beta(k) \quad (12)$$

and can be estimated iteratively using

$$\begin{aligned} v(k+1) &= A(k+1)e^{j(\omega(k+1)\Delta T + \phi)} \\ &= Ae^{j\omega\Delta T}e^{j(\omega k\Delta T + \phi)} = v(k)e^{j\omega\Delta T} \end{aligned} \quad (13)$$

It is important to notice that in normal operating conditions, samples of  $v(k)$  are located on a circle in the complex plane with a constant radius  $A$ , depicted by '+' in Fig. 2. For a constant sampling frequency, the amplitude distribution of  $v(k)$  is rotation invariant, since  $v$  and  $ve^{j\theta}$  have the same distribution for any real  $\theta$ . Since  $v(k)$  is circular, frequency estimation can be performed adequately by a standard linear adaptive filter, such as the CLMS. However, when the three-phase power system deviates from its normal condition, for instance, when the three phase voltages suffer different levels of dips or transients,  $V_a(k), V_b(k), V_c(k)$  are not identical, and samples of  $v(k)$  are not allocated on a circle, as illustrated by the ellipse denoted by '.' in Fig. 2. In this case, the distribution of  $v(k)$  is rotation dependent (noncircular) and the signal is adequately modelled (see the Appendix A for the derivation) only by using the widely linear model in (7), that is

$$v(k) = A(k)e^{j(\omega k\Delta T + \phi)} + B(k)e^{-j(\omega k\Delta T + \phi)} \quad (14)$$

In other words, when  $V_a(k), V_b(k), V_c(k)$  are not identical,  $A(k)$  is no longer a constant, and  $B(k) \neq 0$ , thus introducing a rotation dependent distribution. Hence, in unbalanced conditions,  $v(k)$  exhibits a certain degree of noncircularity, and the model in (13) is no longer adequate. The coefficients of the widely linear signal model in (14) can be adapted using the Augmented CLMS (ACLMS), given by [17]

$$\begin{aligned} \hat{v}(k+1) &= \underbrace{v(k)h(k)}_{\text{standard update}} + \underbrace{v^*(k)g(k)}_{\text{conjugate update}} \\ e(k) &= v(k+1) - \hat{v}(k+1) \\ h(k+1) &= h(k) + \mu e(k)v^*(k) \\ g(k+1) &= g(k) + \mu e(k)v(k) \end{aligned} \quad (15)$$

where  $h(k)$  and  $g(k)$  are respectively the filter weight coefficients corresponding to the standard and conjugate parts at time instant  $k$ ,  $\hat{v}(k+1)$  is the estimate of  $v(k+1)$ ,  $e(k)$  the estimation error, and  $\mu$  the step-size, a small positive constant. The stability conditions of such a closed-loop adaptive system

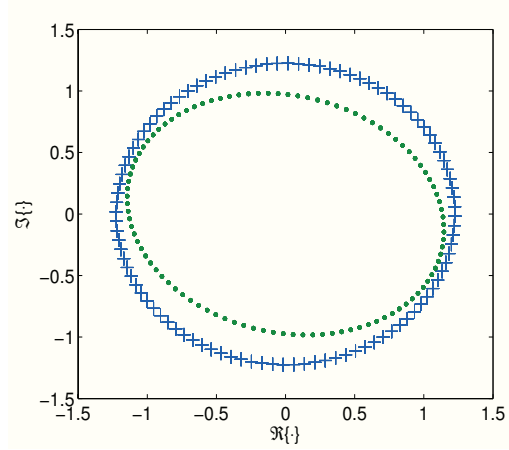


Fig. 2. Circularity via a “real-imaginary” scatter plot in the complex plane. The circle denoted by ‘+’ represents a circular complex-valued signal  $v(k)$  obtained from a balanced situation where  $V_a(k), V_b(k), V_c(k)$  are identical at 1-p.u. and time invariant. The ellipse denoted by ‘.’ represents a noncircular complex-valued  $v(k)$  obtained in an unbalanced condition with  $V_a(k) = 1$ -p.u.,  $V_b(k) = 0.9$ -p.u. and  $V_c(k) = 0.7$ -p.u..

based on ACLMS can be found in [20]; the upper bound for the step-size of ACLMS is roughly half that of CLMS.

From (14) and (15), the estimate  $\hat{v}(k+1)$  becomes

$$\begin{aligned} \hat{v}(k+1) &= A(k)h(k)e^{j(\omega k\Delta T + \phi)} + B(k)h(k)e^{-j(\omega k\Delta T + \phi)} \\ &\quad + A^*(k)g(k)e^{-j(\omega k\Delta T + \phi)} + B^*(k)g(k)e^{j(\omega k\Delta T + \phi)} \\ &= (A(k)h(k) + B^*(k)g(k))e^{j(\omega k\Delta T + \phi)} \\ &\quad + (A^*(k)g(k) + B(k)h(k))e^{-j(\omega k\Delta T + \phi)} \end{aligned} \quad (16)$$

while from (14),  $v(k+1)$  can be re-written as

$$\begin{aligned} v(k+1) &= A(k+1)e^{j\omega\Delta T}e^{j(\omega k\Delta T + \phi)} \\ &\quad + B(k+1)e^{-j\omega\Delta T}e^{-j(\omega k\Delta T + \phi)} \end{aligned} \quad (17)$$

Comparing the ‘standard’, strictly linear parts within (16) and (17), the term  $e^{j\omega\Delta T}$  containing the frequency information can be estimated from

$$e^{j\hat{\omega}\Delta T} = \frac{A(k)h(k) + B^*(k)g(k)}{A(k+1)} \quad (18)$$

while comparing the conjugate parts within (16) and (17), the evolution of the term  $e^{-j\omega\Delta T}$  can be expressed as

$$e^{-j\hat{\omega}\Delta T} = \frac{A^*(k)g(k) + B(k)h(k)}{B(k+1)} \quad (19)$$

thus giving,

$$e^{j\hat{\omega}\Delta T} = \frac{A(k)g^*(k) + B^*(k)h^*(k)}{B^*(k+1)} \quad (20)$$

The assumption held implicitly in frequency estimation by adaptive filtering algorithms is that, at two consecutive time instants,  $A(k+1) \approx A(k)$ , and also  $B(k+1) \approx B(k)$ . This way, (18) and (20) can be respectively simplified into

$$e^{j\hat{\omega}\Delta T} = h(k) + \frac{B^*(k)}{A(k)}g(k) \quad (21)$$

$$e^{j\hat{\omega}\Delta T} = h^*(k) + \frac{A(k)}{B^*(k)}g^*(k) \quad (22)$$

Appendix A shows that the coefficient  $A(k)$  is real-valued whereas  $B(k)$  is complex-valued, and thus  $\frac{B^*(k)}{A(k)} = \left(\frac{B(k)}{A(k)}\right)^*$ . Since (21) should be equal to (22), using  $a(k) = \left(\frac{B(k)}{A(k)}\right)^*$ , we can find the expression for  $a(k)$  by solving the following quadratic equation with complex-valued coefficients

$$g(k)a^2(k) + (h(k) - h^*(k))a(k) - g^*(k) = 0 \quad (23)$$

The discriminant of this quadratic equation is given by

$$\begin{aligned} \Delta &= \sqrt{(h(k) - h^*(k))^2 + 4|g(k)|^2} \\ &= 2\sqrt{-\Im^2(h(k)) + |g(k)|^2} \end{aligned} \quad (24)$$

where the operator  $\Im(\cdot)$  represents the imaginary part of a complex-valued quantity. Since  $a(k)$  is complex-valued, the discriminant is negative, and the two roots become

$$\begin{aligned} a_1(k) &= \frac{-j\Im(h(k)) + j\sqrt{\Im^2(h(k)) - |g(k)|^2}}{g(k)} \\ a_2(k) &= \frac{-j\Im(h(k)) - j\sqrt{\Im^2(h(k)) - |g(k)|^2}}{g(k)} \end{aligned} \quad (25)$$

Observe that the phasor  $e^{j\hat{\omega}\Delta T}$  is estimated either by using  $h(k) + a_1(k)g(k)$  or  $h(k) + a_2(k)g(k)$ . Since the system frequency is far smaller than the sampling frequency, the imaginary part of  $e^{j\hat{\omega}\Delta T}$  can be assumed positive, thus excluding the second solution based on  $a_2(k)$ . The system frequency estimate  $\hat{f}(k)$  is therefore calculated in the form

$$\hat{f}(k) = \frac{1}{2\pi\Delta T} \sin^{-1}(\Im(h(k) + a_1(k)g(k))) \quad (26)$$

The above equation is a generic widely linear extension of the standard linear frequency estimation method, and can be implemented by any type of widely linear adaptive filter. When the system is balanced,  $g(k) = 0$ , and (26) simplifies into the standard linear solution.

#### IV. SIMULATIONS

The strictly linear CLMS [6] and the widely linear ACLMS algorithm were used to estimate the fundamental frequency from both synthetic and real-world voltage signals. The degree of noncircularity in different unbalanced conditions was calculated using the circularity index [16]:

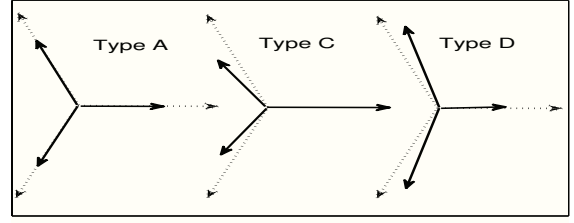
$$\eta = \frac{\tau_v^2}{\sigma_v^2} \quad (27)$$

where  $\sigma_v^2 = E[v(k)v^*(k)]$  is the variance of  $v$ , and  $\tau_v^2 = E[v(k)v^T(k)] = E[|v^2(k)|]$  is the absolute value of the pseudo-variance of  $v$ . This way,  $\eta \in [0, 1]$ , the value of 0 indicating that  $v(k)$  is second order circular (proper), otherwise indicating a second order noncircular (improper)  $v(k)$ .

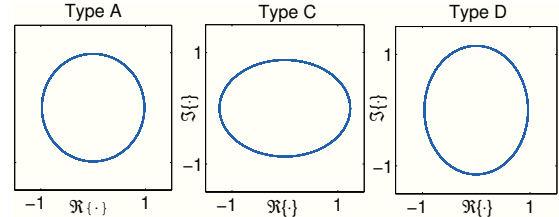
##### A. Synthetic Voltage Sags

The voltage sags most commonly experienced by a three-phase system may be classified into types A, C, and D [21].

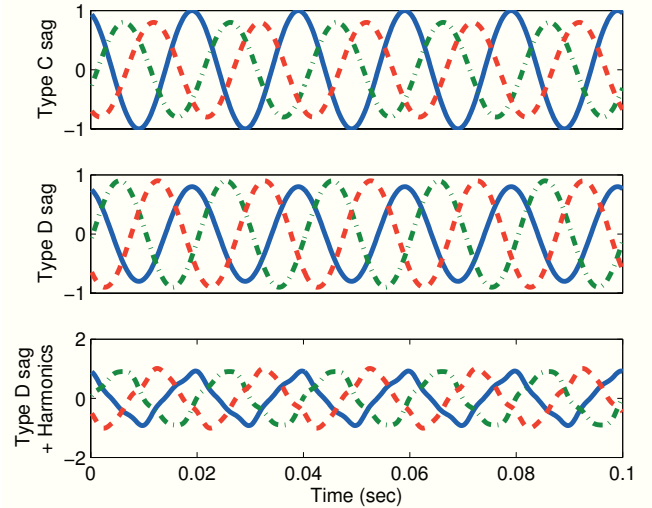
- Type A voltage sag is shown in the left hand part of Fig. 3(a), whereby all the three voltages undergo balanced



(a) Unbalanced voltage sags (dotted line denotes normal operation).



(b) Circularity via a “real-imaginary” plot of sag types A, C and D.



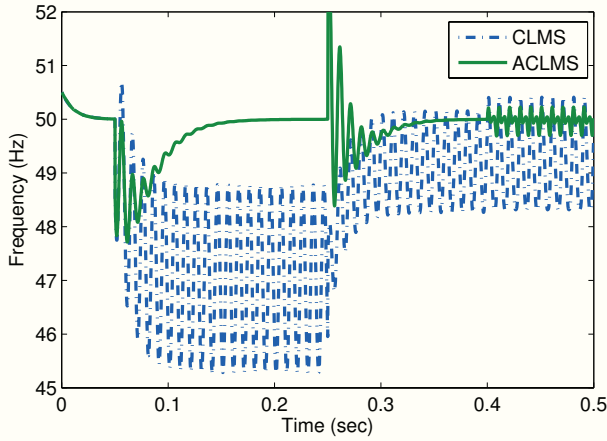
(c) Time series of three-phase voltages for different sag types.

Fig. 3. Waveforms and phase relationships for different voltage sag types.

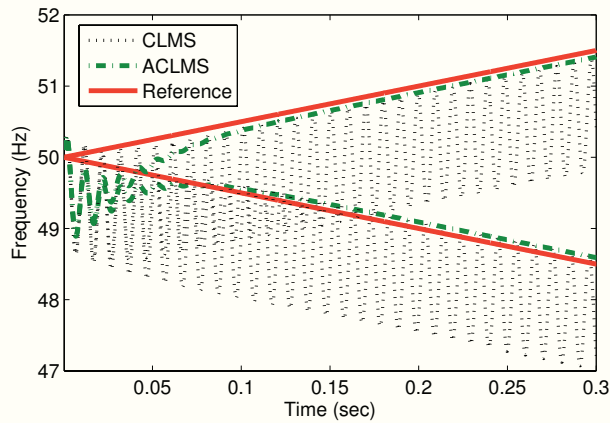
sags at the same magnitude level, and the phase angles between all three phases remain  $120^\circ$  apart.

- Type C and D sags are shown respectively in the middle and right hand part of Fig. 3(a), whereby two phase voltages drop in magnitude at the same rate and also exhibit change in phase angle from their normal position; type C and type D sags may happen in a star-connected and a delta-connected supply system respectively.

Type A sag is also known as symmetrical sag, while the other two are unsymmetrical. A three-phase short circuit or a large motor starting produce symmetrical sags, whereas line-to-ground, phase-to-phase, or two phase-to-ground faults such as lightning, accidents, and energizing of transformers produce unsymmetrical sags. Since type A sag does not alter the circularity of the power system, as shown in Fig. 3(b),



(a) The three-phase power system undergoing three consecutive voltage sags of different natures.



(b) System frequency undergoing the decay and rise at a rate of 5 Hz/sec.

Fig. 4. Frequency estimation using CLMS and ACLMS, for  $\mu = 0.01$ .

the standard linear adaptive estimator is adequate, and in this work, we mainly focus on the latter two unsymmetrical voltage sags of type C and type D exhibiting noncircular amplitude distributions as shown in Fig. 3(b).

The performance of frequency estimation of CLMS and ACLMS under both type C and D sag conditions is shown in Fig. 4(a). Initially, the simulated power system was in its normal operation at 50 Hz with a balanced distortion-free three-phase voltages with unity magnitude. Both algorithms were initialised at 50.5Hz and converged to 50Hz in a very similar way. Then at  $t = 0.05$  s, a type C sag occurred, with a 20% voltage drop and  $10^\circ$  phase angle offset on phases  $v_b$  and  $v_c$ , leading to an unbalanced three-phase power system with a degree of noncircularity  $\eta = 0.3410$  (Fig. 3(b)). There was an inevitable biased oscillation error in CLMS based estimation due to the undermodelling of the system, whereas the advantage of the widely linear ACLMS based estimator in accurately estimating the frequency can be observed after convergence. At  $t = 0.25$  s, a type D sag took place exhibiting a 20% voltage drop at phase  $v_a$  and 10% voltage drop at

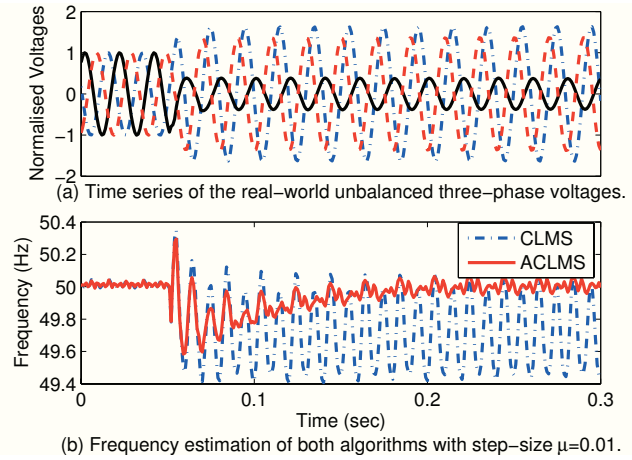


Fig. 5. Frequency estimation for a real-world voltage sag.

both phases  $v_b$  and  $v_c$  together with a  $5^\circ$  phase angle offset, whereby the degree of noncircularity  $\eta$  was 0.1778. Again ACLMS gave an unbiased performance, whereas the CLMS was not adequate. After  $t = 0.4$  s, the unbalanced three-phase voltages were polluted with higher order harmonics; a 10% of the third harmonic and 5% of the fifth harmonic of the fundamental frequency were added into the unbalanced three-phase power system suffering from the same type D sag to give  $\eta = 0.1782$ . The estimated frequency was subject to an oscillatory steady state error; from  $t = 0.4$  s, the ACLMS achieved better performance with a smaller oscillation error at the steady state as compared with CLMS.

In the next case study, the performances of the proposed widely linear ACLMS and the strictly linear CLMS were compared for the case of frequency variation. In Fig. 4(b), the 50 Hz fundamental frequency of the type D unbalanced three-phase voltage arose and decayed at a rate of 5 Hz/sec; the estimated frequency obtained by the ACLMS algorithm followed the true system frequency very closely after an initialisation period of around 0.05 sec, whereas CLMS produced a biased estimation with large variance.

### B. Estimation of Real World Voltage Sags

The real-world three phase voltage with sags was recorded at a 110/20/10kV transformer station. The REL 531 numerical line distance protection terminal, produced by ABB Ltd, was installed in the station and was used to monitor changes in the three 'phase-ground' voltages. The device was set to record whenever the phase voltage value dropped below 90% of its nominal value for longer than 20 ms. The measured three 'phase-ground' voltages with system frequency 50 Hz were sampled at 1 kHz, and were normalised with respect to their normal peak voltage value, as shown in Fig. 5(a). At around  $t = 0.05$  sec, a problem in phase  $v_b$  occurred (shortcut with earth), causing a 30% voltage sag, while the voltages in phases  $v_a$  and  $v_c$  simultaneously experienced respectively 60% and 37% voltage swells, to give a degree of noncircularity of  $\eta = 0.1074$ . The frequency tracking capabilities of the

proposed ACLMS and standard CLMS methods are shown in Fig. 5(b). Both methods provided accurate responses under normal operating conditions, however, as expected, the CLMS failed to deal with the unbalanced situation, whereas the fluctuations of the estimated frequency produced by ACLMS were much lower than those of the CLMS method.

## V. CONCLUSION

We have introduced widely linear estimation of the instantaneous frequency in three-phase power system. The proposed technique, based on the Augmented Complex Least Mean Square (ACLMS) algorithm has been shown to be suitable for both balanced and unbalanced three-phase voltages, and to be robust under different voltage sag conditions. It has been shown that type A sag exhibits rotation invariant (circular) amplitude distribution while type C and type D sags are second order noncircular (improper), for which the standard linear adaptive CLMS based estimator is suboptimal. In addition, the proposed ACLMS based widely linear modelling has also exhibited good tracking ability during dynamic changes in power system, and reduced sensitivity to higher order harmonics as compared to strictly linear estimation.

## APPENDIX A

From the standard three-phase system in (10) and (11), the components  $v_\alpha(k)$  and  $v_\beta(k)$  of the complex voltage  $v(k) = v_\alpha(k) + jv_\beta(k)$ , obtained using the  $\alpha\beta$  transformation, can be derived as

$$\begin{aligned} v_\alpha(k) &= \sqrt{\frac{2}{3}} \left( v_a(k) - \frac{v_b(k)}{2} - \frac{v_c(k)}{2} \right) \\ &= \left( \frac{\sqrt{6}V_a(k)}{3} + \frac{\sqrt{6}(V_b(k) + V_c(k))}{12} \right) \cos(\omega k \Delta T + \phi) \\ &\quad - \frac{\sqrt{2}(V_b(k) - V_c(k))}{4} \sin(\omega k \Delta T + \phi) \end{aligned} \quad (28)$$

$$\begin{aligned} v_\beta(k) &= \sqrt{\frac{2}{3}} \left( \frac{\sqrt{3}v_b(k)}{2} - \frac{\sqrt{3}v_c(k)}{2} \right) \\ &= -\frac{\sqrt{2}(V_b(k) - V_c(k))}{4} \cos(\omega k \Delta T + \phi) \\ &\quad + \frac{\sqrt{6}(V_b(k) + V_c(k))}{4} \sin(\omega k \Delta T + \phi) \end{aligned} \quad (29)$$

Given that

$$\begin{aligned} \cos(\omega k \Delta T + \phi) &= \frac{e^{j(\omega k \Delta T + \phi)} + e^{-j(\omega k \Delta T + \phi)}}{2} \\ \sin(\omega k \Delta T + \phi) &= \frac{e^{j(\omega k \Delta T + \phi)} - e^{-j(\omega k \Delta T + \phi)}}{2j} \end{aligned} \quad (30)$$

the complex-valued  $v(k)$  can be written in the form of a standard part (left hand term) and a conjugate part (right hand term) as  $v(k) = v_\alpha(k) + jv_\beta(k)$ , that is

$$v(k) = A(k)e^{j(\omega k \Delta T + \phi)} + B(k)e^{-j(\omega k \Delta T + \phi)} \quad (31)$$

where

$$\begin{aligned} A(k) &= \frac{\sqrt{6}(V_a(k) + V_b(k) + V_c(k))}{6} \\ B(k) &= \frac{\sqrt{6}(2V_a(k) - V_b(k) - V_c(k))}{12} - \frac{\sqrt{2}(V_b(k) - V_c(k))}{4}j \end{aligned}$$

Augmented complex statistics [16], [18] shows that  $v(k)$  is second order circular with rotation invariant probability density function in the complex plane if  $B(k)$  vanishes and  $A(k)$  is a constant, which can only be achieved when  $V_a(k), V_b(k), V_c(k)$  are identical at each time instant, when (31) simplifies into (13). In unbalanced conditions,  $A(k)$  is real-valued, but  $B(k) \neq 0$  and can be complex-valued, resulting in a second order noncircular (improper)  $v(k)$ .

## REFERENCES

- [1] M. S. Sachdev and M. M. Giray, "A least square technique for determining power system frequency," *IEEE Trans. Power App. Syst.*, vol. PAS-104, no. 5, pp. 1025–1038, 1983.
- [2] J. Yang and C. Liu, "A precise calculation of power system frequency," *IEEE Trans. Power Del.*, vol. 16, no. 3, pp. 361–366, 2001.
- [3] V. Eckhardt, P. Hippe, and G. Hosemann, "Dynamic measuring of frequency and frequency oscillations in multiphase power systems," *IEEE Trans. Power Del.*, vol. 4, no. 1, pp. 95–102, 1989.
- [4] E. Clarke, *Circuit Analysis of A.C. Power Systems*, New York: Wiley, 1943.
- [5] P. Rodriguez, J. Pou, J. Bergas, J. I. Candela, R. P. Burgos, and D. Boroyevich, "Decoupled double synchronous reference frame PLL for power converter control," *IEEE Trans. Power Electron.*, vol. 22, no. 2, pp. 584–592, 2007.
- [6] A. K. Pradhan, A. Routray, and A. Basak, "Power system frequency estimation using least mean square technique," *IEEE Trans. Power Del.*, vol. 20, no. 3, pp. 761–766, 2005.
- [7] P. K. Dash, A. K. Pradhan, and G. Panda, "Frequency estimation of distorted power system signals using extended complex Kalman filter," *IEEE Trans. Power Del.*, vol. 14, no. 3, pp. 761–766, 1999.
- [8] M. Akke, "Frequency estimation by demodulation of two complex signals," *IEEE Trans. Power Del.*, vol. 12, no. 1, pp. 157–163, 1997.
- [9] J. L. Duran-Gomez, P. N. Enjeti, and B. O. Woo, "Effect of voltage sags on adjustable speed drives – a critical evaluation and approach to improve its performance," *Proc. 14th Annu. Applied Power Electronics Conf. Expo.*, vol. 2, pp. 774–780, 1999.
- [10] D. Beeman, *Industrial Power System Handbook*, McGraw-Hill, 1955.
- [11] H. S. Song and K. Nam, "Instantaneous phase-angle estimation algorithm under unbalanced voltage-sag conditions," *IEE Proc. Gener. Transm. Distrib.*, vol. 147, no. 6, pp. 409–415, 2000.
- [12] M. D. Kušljević, J. J. Tomić, and L. D. Jovanović, "Frequency estimation of three-phase power system using weighted-least-square algorithm and adaptive FIR filtering," *IEEE Trans. Instrum. Meas.*, vol. 57, no. 10, pp. 322–329, 2010.
- [13] M. Mojiri, D. Yazdani, and A. Bakhshai, "Robust adaptive frequency estimation of three-phase power system," *IEEE Trans. Instrum. Meas.*, vol. 59, no. 7, pp. 1793–1802, 2010.
- [14] B. Picinbono and P. Chevalier, "Widely linear estimation with complex data," *IEEE Trans. Signal Process.*, vol. 43, no. 8, pp. 2030–2033, 1995.
- [15] P. J. Schreier and L. L. Scharf, "Second-order analysis of improper complex random vectors and process," *IEEE Trans. Signal Process.*, vol. 51, no. 3, pp. 714–725, 2003.
- [16] D. P. Mandic and S. L. Goh, *Complex Valued Nonlinear Adaptive Filters: Noncircularity, Widely Linear and Neural Models*, John Wiley & Sons, 2009.
- [17] S. Javidi, S. L. Goh M. Pedzisz, and D. P. Mandic, "The augmented complex least mean square algorithm with application to adaptive prediction problems," *Proc. 1st IARP Workshop Cogn. Inform. Process.*, pp. 54–57, 2008.
- [18] B. Picinbono, "On circularity," *IEEE Trans. Signal Process.*, vol. 42, no. 12, pp. 3473–3482, 1994.
- [19] Y. Xia, B. Jelfs, M. M. Van Hulle, J. C. Principe, and D. P. Mandic, "An augmented echo state network for nonlinear adaptive filtering of complex noncircular signals," *IEEE Trans. Neural Netw.*, vol. 22, no. 1, pp. 74–83, 2011.
- [20] S. C. Douglas and D. P. Mandic, "Performance analysis of the conventional complex LMS and augmented complex LMS algorithms," *Proc. IEEE Int. Conf. Acoust., Speech Signal Process.*, pp. 3794–3797, 2010.
- [21] M. H. J. Bollen, "Voltage sags in three-phase systems," *IEEE Trans. Power Eng. Rev.*, vol. 21, no. 9, pp. 8–15, 2001.